dissociation energy of Mn_2^+. The largest value in Table I is 1.39 eV obtained at 514 nm. This value is an average of four measurements with a statistical error of ±0.03 eV. The dissociation energy of Mn_2^+ is thus ≥1.39 eV (32 kcal mol^{-1}). From this result we derive a value for the adiabatic ionization potential for Mn_2 of $IP(Mn_2) \leq 6.47$ eV from the relationship

$$IP(Mn_2) = IP(Mn) + D°_0(Mn-Mn) - D°_0(Mn^+-Mn) \quad (4)$$

using IP(Mn) = 7.43 eV[19] and $D°_0(Mn_2) = 0.43$ eV.[7]

We assume in the above discussion that we are not photodissociating electronically excited Mn_2^+. From the observation of the "metastable" dissociation we know that a small fraction of the Mn_2^+ beam is in a long-lived excited electronic state. However, to be important in the photodissociation the electronically excited Mn_2^+ ions would have to make up a substantial proportion of the Mn_2^+ beam. There is no evidence from other studies that formation of Mn_2^+ from $Mn_2(CO)_{10}$ results in a substantial population in electronically excited states.[10,11] There appear to be no spin or symmetry restrictions to producing ground-state Mn_2^+ from $Mn_2(CO)_{10}$. Finally, the experiments with the buffer gas provide some evidence that we are sampling ground electronic state ions, although it is not clear how rapidly N_2 would quench electronically excited Mn_2^+.

The value for the metal-metal bond energy derived above $D°_0(Mn^+-Mn) \geq 1.39$ eV is substantially larger than that obtained by Ervin et al.[10] from the threshold for collision-induced dissociation of Mn_2^+. They derived a value of 0.85 ± 0.2 eV for the dissociation energy. In their experiment it is necessary to generate vibrationally cold ground-state ions, which they attempted to do using low-energy electron impact on $Mn_2(CO)_{10}$. It seems likely that a small fraction of their Mn_2^+ ions was vibrationally excited resulting in a low value for the dissociation energy of Mn_2^+ in their study.

V. Conclusions

The dimanganese ion from electron impact on $Mn_2(CO)_{10}$ photodissociates in the visible region of the spectrum. The photofragment relative kinetic energy distributions show that ground and excited electronic state products are produced and that some of the dimanganese ions are internally excited. Studies with N_2 buffer gas suggest that collisions with N_2 remove the internal energy from Mn_2^+. The photofragment angular distributions for both ground and excited electronic state products are characterized by an asymmetry parameter of $\beta = 0.4 \pm 0.1$ which suggests that photodissociation of Mn_2^+ occurs via an intermediate-bound excited state(s) which predissociates by a curve crossing mechanism. Analysis of the kinetic energy thresholds in the photofragment distributions leads to a rigorous lower limit for the metal-metal bond energy in Mn_2^+ of $D°_0(Mn^+-Mn) \geq 1.39$ eV and an adiabatic ionization potential for Mn_2 of $IP(Mn_2) \leq 6.47$ eV (assuming $D°_0(Mn_2) = 0.43$ eV).[7] The dissociation energy is larger than previously reported by Ervin et al. (0.85 ± 0.2 eV)[10] probably because their ions were internally excited.

Acknowledgment. We gratefully acknowledge the support of the Air Force Office of Scientific Research under Grant AFOSR82-0035 and the National Science Foundation under Grant CHE80-20464. We are also grateful for a number of useful discussions with Dr. Tony O'Keefe. Finally, We acknowledge useful conversations with Professor P. Armentrout on details of our source design.

The Electronic Spectrum of Cytosine

František Žaloudek, Joel S. Novros, and Leigh B. Clark*

Contribution from the Department of Chemistry, University of California, San Diego, La Jolla, California 92093. *Received October 9, 1984*

Abstract: Polarized reflection spectra in the range 360 to 135 nm taken from the (100) and (001) faces of single crystals of cytosine monohydrate have been interpreted through the Kramers-Kronig transformation in order to assign the polarization directions of six electronic transition moments of cytosine. Published linear dichroism studies of cytosine along with other crystal work are used to resolve the usual ambiguity in the interpretation of crystal spectra for the lowest three $\pi \rightarrow \pi^*$ transitions. An oriented gas analysis of the crystal spectra yield the following transition moment directions: $\theta_I = +6°$, $\theta_{II} = -46°$, $\theta_{III} = +76°$, $\theta_{IV} = -27°$ or 86°. Crystal field effects are considered in the dipole approximation in an effort to extract free molecule properties from the crystal data. Exciton mixing causes no large directional changes in moment directions; however, band components along the different crystal axes can show energy shifts of the order of 5000 cm^{-1}. Two higher energy features at 165 and 150 nm are discussed. The absorption spectrum polarized perpendicular to the molecular planes (obtained from reflection data taken from the (010) crystal face) shows no compelling evidence for an $n \rightarrow \pi^*$ transition at wavelengths longer than 225 nm.

There is at present considerable interest in the calculation of the optical properties of nucleic acids and polynucleotides.[1-3] Work is being directed in order to develop trustworthy ways of calculating the linear dichroism (LD) and circular dichroism (CD) for any particular polymer sequence and conformation. If the program is successful, then the comparison between such calculations and experimental CD and LD spectra will be useful in conformational deductions. Such studies, when taken together with structural information obtained with other methods, for example, NMR,[4] will surely reveal the physical nature and transformations of these polymers. Common to all approaches aimed at the optical properties is the need to understand the electronic states of the monomeric chromophores involved. Of special significance is a knowledge of the various monomer transition moment directions, for it is the mutual orientations of these moments which are of vital importance in the determination of the optical properties of the polymers. The experimentally known transition moment directions are either used directly in the calculations or employed to adjust and scale theoretically determined LCAO monopoles.

(1) See, for example the following review: Woody, R. W. *J. Polym. Sci.* **1977**, *12*, 181.
(2) Rizzo, V.; Schellman, J. A. *Biopolymers* **1984**, *23*, 435 and references therein.
(3) Matsuoka, Y.; Norden, B. *Biopolymers* **1983**, *22*, 1731.
(4) For a review of this important area see: Kearns, D. R. *Crit. Rev. Biochem.* **1984**, *15*, 237.

0002-7863/85/1507-7344$01.50/0

Unfortunately, after two decades of work, the necessary transition moment information for the purine and pyrimidine bases remains somewhat meager. With the exception of that for guanine,[5] the existing data that have been gleaned through single crystal absorption[6-8] and reflection,[9-13] fluorescence polarization,[14] and linear dichroism methods[15-17] cover only the lowest energy one or two transitions. Recent work on extending CD measurements into the vacuum ultraviolet region has emphasized the importance of the higher energy transitions in the range 180–200 nm.[18-21] Knowledge of these transition moments is vital, not only for interpreting the strong CD bands in the region but also in dealing with the effects of interstate mixing on all the transitions.

The present work is aimed at providing transition moment data for cytosine throughout the important spectral range of 140 to 300 nm by examining the spectra of single crystals of cytosine monohydrate. We have attempted to address the important concern regarding the effects of exciton mixing on the polarization directions obtained from crystal spectra by carrying through calculations aimed at extracting free molecule properties from the crystal spectra.

It is felt that these data can be used not only with the earlier results for guanine[5] in the interpretation of the many forms involving just G and C, e.g., poly(dG·dC)·poly(dG·dC),[22] but also for various calculations on polymer forms of C itself. In addition, when combined with recent results[13] for protonated cytosine, C^+, they should provide the necessary input for calculations of the semiprotonated polymer form poly(C)·poly(C^+) which occurs at pH 4.[1] The fact that cytosine forms a large number of polymers may be used to lever successes and failures out of the theoretical approaches. At least that is our hope. It has been suggested that 1-methylcytosine should serve as a better model compound than cytosine. Unfortunately the triclinic crystal structure of 1-methylcytosine complicates any spectroscopic investigation to such an extent as to render it the second choice in this regard.

The strategy used here is to employ the absorption curves for light polarized along various axes of single crystals of cytosine monohydrate in the derivation of transition moment directions. The absorption curves are obtained from experimental polarized reflection spectra through Kramers–Kronig analysis and are further analyzed in two ways. First the usual oriented gas analysis is carried through. Subsequently, crystal field effects are considered in an attempt to extract free molecule properties from the crystal spectra.

It must be admitted at the outset that the bands of cytosine are badly overlapped and that considerable ambiguity occurs in the resolution of the spectra into individual band components. We feel that it is valuable, nevertheless, to make an attempt at an interpretation and assignment, for band assignments even carrying appreciable but identified uncertainty are better than no assignments whatsoever.

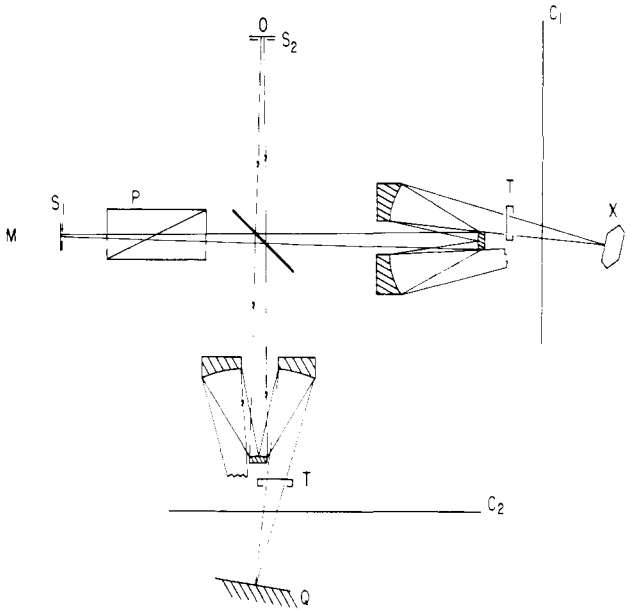

Figure 1. Optical layout of the reflection spectrophotometer. M is the monochromator, S_1 and S_2 are slits, and P is a quartz Rochon polarizer. The T are slots which accept a portion of the radiation exiting the Cassegrainian microscope objectives. C_1 and C_2 are choppers while X and Q are the crystal and standard quartz reference, respectively. D represents a photomultiplier tube.

Experimental Section

Crystal Preparation. Single crystals of cytosine monohydrate were grown by slow evaporation from aqueous solution. Clear crystals showing smooth, shiny faces and uniform extinction were easily obtained. The principal faces that developed were identified by morphologic examination and included the unit cell planes of (001), (100), and (010). Linear dimensions were of the order of several millimeters. No photodamage was observed during the course of these measurements.

Reflection Spectrophotometers. For the visible and ultraviolet (650–185 nm) a 1-m monochromator (McPherson, Model 2051) was employed with a quartz Rochon polarizer (Karl Lambrecht) to direct monochromatic radiation through a silica plate beam splitter into a Cassegrainian (reflecting) microscope objective (Beck, 15×) as shown in Figure 1. The polarizer was positioned so that the ordinary ray was horizontally polarized. Only a thin, vertical slice of the light coming to the crystal from the upper portion of the Cassegrainian was accepted so as to (1) reduce the angle of incidence to about ±1°, (2) eliminate depolarization effects in the reflecting objective, and (3) ensure that no longitudinal component of polarization would reach the crystal. When a crystal face at the point of focus is made normal to the incident light, then the reflected beam retraces its path to the beam splitter, whereupon a portion is deflected vertically to form an image of the monochromator slit at a second slit positioned just before a photomultiplier tube. The second slit serves to reduce the stray light reaching the detector and blocks off the extraordinary ray (vertical polarization) which by this point is deviated by about 5 mm from the ordinary ray. It should be mentioned that the beam splitter serves as a fairly efficient polarizing element in its own right, since radiation is incident at an angle not far from Brewster's angle for quartz.

By using the portion of the beam initially directed downward from the beam splitter through a second Cassegrainian onto a standard reference reflector (polished silica plate), a reference signal can be directed back to the detector. Both beams experience one pass and one reflection at the beam splitter.

The two beams are separately chopped at unrelated frequencies, and the signal from the photomultiplier tube is fed to two lock-in amplifiers for separation and amplification of the individual components. The ratio of these signals is then recorded.

The signal reflected from a second silica plate identical with the reference piece is measured in order to obtain the instrument calibration factor, I_Q^{Ref}/I_Q, at each wavelength. The reflection signal from a crystal is then found by substituting the crystal for the second silica plate and recording the ratio I_{xtal}/I_Q^{Ref}. Finally, the absolute reflectivity of the crystal is given by

(5) Clark, L. B. *J. Am. Chem. Soc.* **1977**, *99*, 3934.
(6) 9-Methyladenine: Stewart, R. F.; Davidson, J. *J. Chem. Phys.* **1963**, *39*, 255.
(7) 1-Methyluracil: Eaton, W. A.; Lewis, T. P. *J. Chem. Phys.* **1970**, *53*, 2164.
(8) Cytosine·H_2O: Lewis, T. P.; Eaton, W. A. *J. Am. Chem. Soc.* **1971**, *93*, 2054.
(9) Cytosine, 1-methylcytosine: Callis, P. R.; Simpson, W. T. *J. Am. Chem. Soc.* **1970**, *92*, 3593.
(10) Adenine·HCl: Chen, H. H.; Clark, L. B. *J. Chem. Phys.* **1973**, *58*, 2593.
(11) Thymine: Anex, B. G.; Fucaloro, A. F.; Durra-Ahmed, A. *J. Phys. Chem.* **1975**, *79*, 2636.
(12) 6-Azauracil: Brown, J. N.; Trefonas, L. M.; Fucaloro, A. F; Anex, B. G. *J. Am. Chem. Soc.* **1974**, *96*, 1597.
(13) Cytosine·HBr: Clark, L. B. *J. Am. Chem. Soc.*, submitted for publication.
(14) See the following review: Callis, P. R. *Ann. Rev. Phys. Chem.* **1983**, *34*, 329.
(15) Fucaloro, A. F.; Forster, L. S. *J. Am. Chem. Soc.* **1971**, *93*, 6443.
(16) Bott, C. C.; Kurucsev, T. *Spectrosc. Lett.* **1977**, *10*, 495.
(17) Matsuoka, Y.; Norden, B. *J. Phys. Chem.* **1982**, *86*, 1378.
(18) Johnson, W. C. *Annu. Rev. Phys. Chem.* **1978**, *29*, 93.
(19) Sprecher, C. A.; Johnson, W. C. *Biopolymers* **1977**, *16*, 2243.
(20) Sutherland, J. C.; Griffen, K. P.; Keck, P. C.; Takacs, P. Z. *Proc. Natl. Acad. Sci. U.S.A.* **1981**, *78*, 4801.
(21) Sutherland, J. C.; Griffen, K. P. *Biopolymers* **1983**, *22*, 1445.
(22) Pohl, F. M.; Jovin, T. M. *J. Mol. Biol.* **1972**, *67*, 375.

$$R_{xtal} = (I_{xtal}/I_Q^{Ref})(I_Q^{Ref}/I_Q)R_Q$$

where R_Q is the absolute reflection of quartz calculated from known indices of refraction.[23] The crystal is mounted on a goniometer head attached to translation and rotation stages. The chosen face is made normal to the incident beam simply by searching for a maximum in the reflected signal.

The instrument used for the vacuum UV region is again similar in design. A McPherson 1-M vacuum monochromator (Model 225) is employed with a MgF_2 Rochon polarizer (Karl Lambrecht). The beam splitter consists of two parallel LiF plates. The crystal is mounted in a dry nitrogen flushed chamber which is separated from the evacuated optical train by a LiF window. The total path length of the radiation through the nitrogen gas is about 3 mm. A sodium salicylate coated photomultiplier tube serves as the detector. Measurements to 135 nm are made in a point-by-point fashion with use of the emission lines of a Hinterrigger H_2–D_2 lamp. Polished LiF plates are used as the standard and reference reflectors.[24]

Reflection Spectra. Reflection spectra for radiation polarized along the two principal optical directions of both the (001) and (100) crystal faces were recorded for a number of crystals. Since the *b* axis is common in both faces, the three spectral curves representing the reflection spectra polarized parallel to the *a*, *b*, and *c* axes constitute the results. Data were collected between 360 and 135 nm and are shown in Figure 2 along with the aqueous solution spectrum for comparison. As expected, the *b* axis spectrum was found to be the same for the (001) and (100) faces.

Absorption Spectra. Absorption spectra corresponding to the recorded reflection curves are obtained through the Kramers–Kronig transformation. Equations for this transformation have been given before.[25] The exact evaluation of the phase shift $\theta(\omega)$ from which the absorption index $k(\omega)$ is calculated requires a numerical integration over the entire frequency domain. Even though the experimental frequency range is limited, a satisfactory procedure is to construct reflectivity curves for the unmeasured IR and extreme UV regions which can then be systematically varied in a trial and error fashion until the computed absorption coefficients are essentially zero throughout the known transparent region. The low-frequency region was constructed in the present study by smoothly extending the data from 360 nm through the visible and infrared to zero frequency. It was demanded that these curves pass through the reflectivities at 589 nm calculated from index of reflection data.[8,26] [See small circles in Figure 2.] The three derived absorption curves are given as the solid curves in the lower frames of Figure 2.

Considerable faith in the accuracy of these procedures can be gained by comparing the results obtained through transformation of reflection data to those obtained by direct absorption measurements where available. In this regard we show for comparison the *b* axis absorption spectrum measured directly by Lewis and Eaton.[8] For this lowest energy transition, we derive a maximum extinction along the *b* axis of 18 200 while the value obtained by direct absorption is 16 600 and carries a stated uncertainty (due to thickness determination) of ±10%. Again, almost quantitative agreement in peak height is obtained in a similar comparison for the first transition of 1-methyluracil.[27]

Crystal Structure. The crystal structure of cytosine monohydrate has been the subject of considerable study and refinement.[28–30] The unit cell is monoclinic (space group $P2_1/c$) and contians four cytosine molecules. The projection of the unit cell onto the (001) plane is shown in Figure 3. The different sites are interchanged by factor group operations and are related through the following equivalent points: $1(x,y,z)$, $2(\bar{x},\bar{y},\bar{z})$, $3(\bar{x},{}^1/_2 + y,{}^1/_2 - z)$, $4(x,{}^1/_2 - y,{}^1/_2 + z)$.

The dichroic ratio (i.e., the ratio of absorption intensities along two different crystal axes) represents the ratio of the squared vector components of the projection of a given transition moment. If the transition moment is not severely restricted by symmetry considerations, there will be at least two molecular directions consistent with a given dichroic ratio. For the system studied here, the two choices correspond to identical possibilities in all four sites, so that we need to focus attention only on a representative site in the following analyses. The projections of such a representative molecule are shown as insets in Figure 2. It should be mentioned that the crystal structure of cytosine monohydrate is such as not to permit the resolution of this type of ambiguity, and one must seek other evidence or data in order to make final assignments.

Oriented Gas Model

The goal of this work is to obtain transition moment directions of the free cytosine molecule. Although the mixing of states due to crystal interactions alters dichroic ratios and consequently the apparent transition moment directions, it is advisable intially to ignore such effects and work up the data within the framework of the oriented gas model. All previous interpretations of the cytosine crystal spectra have used this approach. Furthermore, as we shall see, when the effects of the crystal field are taken into account, the changes which occur are not large enough to overturn the general conclusions obtained by the oriented gas analysis.

Transition moments for a molecule exhibiting only planar symmetry (space group C_s) will be directed perpendicularly to the plane ($n \rightarrow \pi^*$) or will occur somewhere in the molecular plane ($\pi \rightarrow \pi^*$). For the latter type, we seek the in-plane orientation relative to some arbitrary reference axis. The reference axis is chosen according to the DeVoe–Tinoco convention to be the N_1–C_4 axis, and positive angles, θ, are measured toward N_4 as shown in Figure 4. We further define an out-of-plane angle, ϕ, as positive when the head of the vector is elevated out of the plane of the molecule as shown in Figure 4.

The aqueous solution absorption spectrum (Figure 2) exhibits four features. There are two maxima at 266 and 197 nm and two inflections at 230 and 212 nm. These four features correspond to the principal, in-plane polarized bands for which this paper mostly pertains. The spectrum of an evaporated film of cytosine in the vacuum UV region shows additional maxima at 165 and 150 nm.[31] The bands will be labeled serially with Raman numerals, I–VI as shown in Figure 2.

Turning now to the derived crystal absorption spectra, we see that with the exception of I there are immediate difficulties in the association of individual components with given transitions. For example, the positions of the peaks in the region expected for IV varies by 6000 cm^{-1} from axis to axis. Individual components are badly overlapped so that resolution into components will necessarily be somewhat arbitrary. The tactic employed here was to demand plausible band shapes and to carry out the resolutions in a fashion which seemed most straightforward while keeping an eye on the presumed in-plane nature of the transitions and all other available information.

The case which emerged as the most likely in our judgment is shown as the dotted sets of band components in Figure 2. The fact that the energies of the components of transition IV (as drawn) shift considerably from one axis to the other agrees almost quantitatively with calculated Davydov splittings to be discussed later. The components of I and IV can be resolved with relatively little uncertainty. What then remains represents the overlapped components of II and III, and resolution into individual components here is much less certain. Of course, such increased ambiguity simply carries through to a larger uncertainty for the final transition moment directions.

Transition I. The lowest energy band has been examined in two previous crystal studies and there is little doubt about its general assignment. Callis and Simpson[9] using an approximate, inductive method derived the two possible, in-plane directions from their reflection spectra of the (001) face of cytosine monohydrate to be +9° and +51°. The +9° value was chosen by requiring qualitative consistency with data taken from 1-methylcytosine crystals, and the estimated uncertainty based on their methodology was given as ±10°. Lewis and Eaton,[8] using direct absorption measurements through the (100) plane of cytosine monohydrate, obtained the possible in-plane angles of +10° and +52° and chose +10° to agree with Callis and Simpson. The resolved band components for I given in Figure 2 yield in-plane choices of +6° and +54°, and the +6° value is selected in conformance with the previous work.

Turning now to the important results from linear dichroism studies of cytosine (and some related compounds)[16,17] dissolved

(23) Maliston, I. H. *J. Opt. Soc. Am.* **1965**, *55*, 1205.
(24) Roessler, D. M.; Walker, W. C. *J. Opt. Soc. Am.* **1967**, *57*, 835.
(25) Chen, H. H.; Clark, L. B. *J. Chem. Phys.* **1969**, *51*, 1862.
(26) Hendricks, S. B. *J. Am. Chem. Soc.* **1935**, *57*, 552.
(27) Novros, J. S.; Clark, L. B. *J. Am. Chem. Soc.*, submitted for publication.
(28) Jeffrey, G. A.; Kinoshita, Y. *Acta Crystallogr.* **1963**, *16*, 20.
(29) McClure, R. J.; Craven, B. M. *Acta Crystallogr.* **1973**, *B29*, 1234.
(30) Neidle, S.; Achari, A.; Rabinovitch, M. *Acta Crystallogr.* **1976**, *B32*, 2050.
(31) Raksanyi, K., Foldvary *Biopolymers* **1978**, *17*, 887.

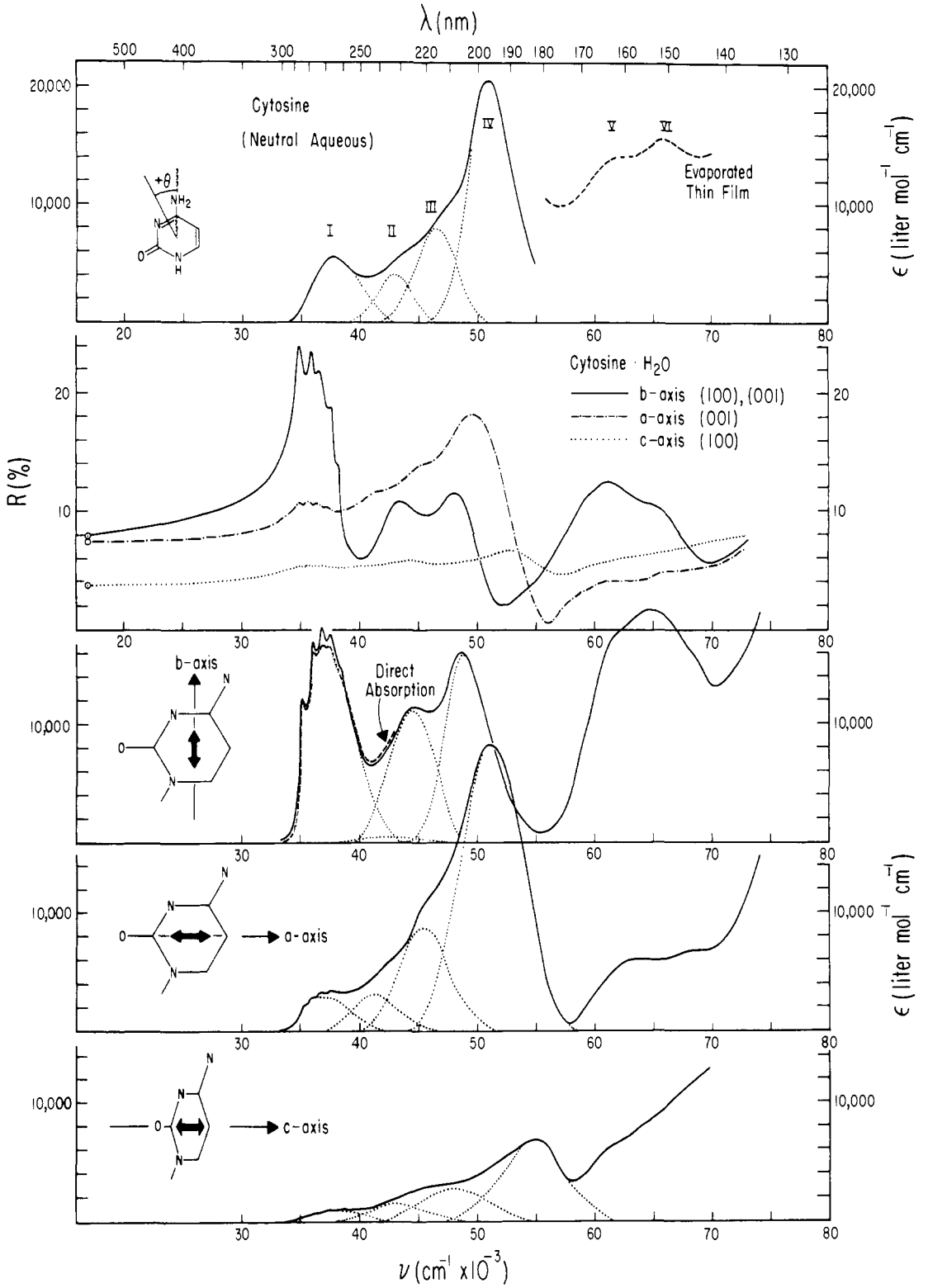

Figure 2. Collected spectra of cytosine. [Top] Aqueous solution absorption spectrum resolved into four band components. The dashed curve is the absorption due to a thin evaporated film (redrawn from ref 31). [Second from top] Reflection spectra for light polarized along the *a* and *b* axes of (001) and the *b* and *c* axes of (100). The small circles at 589 nm are reflectivities calculated from known indices of refraction. [Lower three frames] Absorption spectra for light polarized along the *b*, *a*, and *c* crystal axes derived by Kramers–Kronig analysis of the corresponding reflection spectra. The dotted bands are the particular choice of resolutions into components used in the oriented gas analysis discussed in the text. The dashed curve is redrawn from the results of a direct absorption study (ref 8). The projections of a representative molecule onto the faces involved are shown as insets by the absorption curves.

in stretched poly(vinyl alcohol) films we see an apparent lack of agreement among the methods as indicated in Figure 5. In the stretched film method, some sort of ordered distribution of molecules about the stretching axis occurs. The nature of the ordering parameters is determined from experimental infrared dichroism of various vibrational modes. With use of these derived ordering parameters, the results in the UV can be interpreted in terms of some average orientational axis of the molecules along the stretching direction. As in crystal work there will be two possible in-plane transition moment directions consistent with a given linear dichroism. These directions are aimed equally to either side of the projection of the effective orientation axis onto the

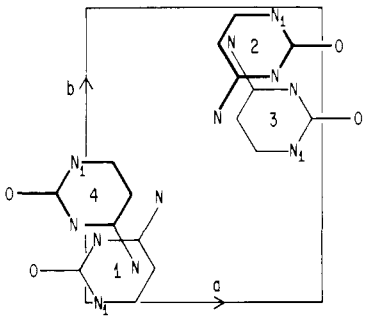

Figure 3. Projection of the four cytosine molecules of the unit cell onto the (001) face. The planes of these molecules lie within 1° from the *b* axis and make an angle of 62° with respect to the *c* axis. The individual unit cell sites are labeled 1 to 4.

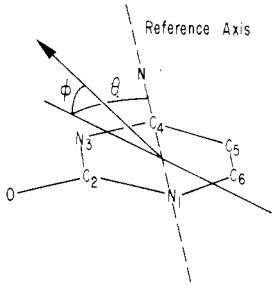

Figure 4. Choice of angles in cytosine. The azimuthal angle θ is measured from the N_1–C_4 axis toward N_3 according to the DeVoe–Tinoco convention. The out-of-plane (elevation) angle ϕ is as shown.

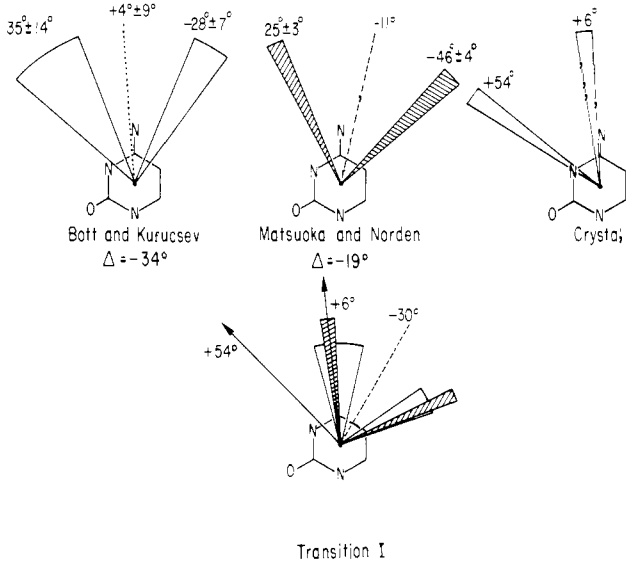

Figure 5. Comparison of stretched film and crystal oriented gas results for transition I. [Top] Comparison of two linear dichroism studies of cytosine in stretched poly(vinyl alcohol) (ref 16 and 17) and the oriented gas crystal result. [Bottom] Coincidence of choices when a −30° effective orientation axis is used for the stretched film work. The necessary angular adjustments are indicated as Δ (see text).

molecular plane. Since the choice of the effective orientation axis is heavily dependent on the results from the IR dichroism studies, the actual in-plane angles θ are susceptible to any errors or difficulties in the IR interpretations. However, the relative angles between successive transition moments are independent of the choice of orientational parameters.

The orientations of the molecules in the crystal are, of course, perfectly known. We ask if there is an effective orientation axis for the stretched film work that would harmonize those results with the crystal outcome? The answer is yes. If the projection of this axis onto the plane is rotated −19° in the work of Matsuoka and Norden[17] and −34° in the work of Bott and Kurucsev,[16] then not only do the corresponding choices in the two LD studies

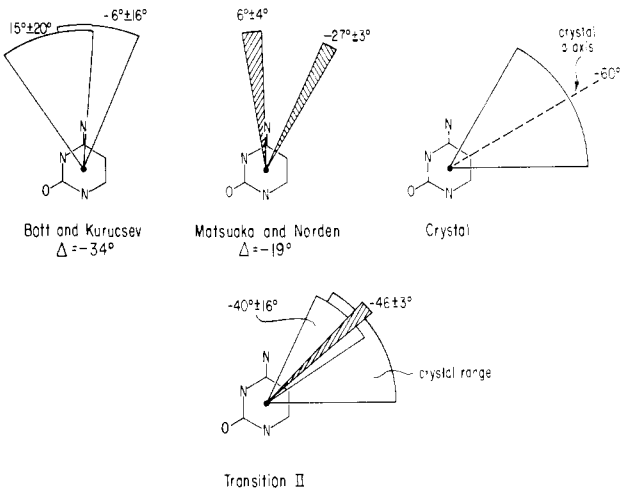

Figure 6. Comparison of stretched film and crystal oriented gas result for transition II. [Top] Comparison of the two linear dichroism studies of cytosine in stretched poly(vinyl alcohol) (ref 16 and 17) and the oriented gas crystal result. The large uncertainty of the crystal result arises from the fact that II_b is completely obscured in the crystal spectrum (see text). [Bottom] Coincidence of choices when a −30° effective orientation axis is used for the stretched film work.

coincide but one of the mutual choices appears at about +6°. In addition, the projection of the effective orientation axis onto the molecular plane occurs at −30° for both film studies. A possible explanation for the disparity may be that the polarizations of the IR bands are different from those anticipated for an independent oscillator model. Appreciable coupling between the infrared bands could lead to changes of the observed magnitude. In this regard a normal coordinate analysis of cytosine would seem to be in order. Our point of view, nevertheless, requires that the results of the two LD studies agree with each other and with the present crystal study.

The stretched film work is important, for (just as in crystal results) it provides a pair of possible transition moment directions for each band. Since the molecular orientations in the crystal are in general different from those in the stretched film, only a single coincident choice among the two pairs of directions for each band should occur when the results of the two methods are compared.

The isotropic oscillator strength calculated from the crystal spectra is 0.14 and compares with the solution spectrum value of 0.13. The slight increase is consistent with the calculated hyperchromic effect on the dominant *b* axis component owing to crystal interactions (vide infra).

Transition II. The second transition is a difficult case, for a distinct feature is observed only in the *a* axis spectrum. Presumably, any *b* axis component is weak and completely obscured by the adjacent, strong bands. The situation is made worse by the apparent shift to lower energy of III_b. If II_b has zero intensity, then an in-plane II is polarized at $\theta = -60°$. However, there is considerable uncertainty in this regard because a modest II_b component could easily be present. A reasonable estimate of this uncertainty is about ±30°.

The result for II given by Callis and Simpson,[9] we believe, is not right because their analysis presumed the reflection band at 44 000 cm^{-1} (near the terminus of their measurements along the *b* axis) represented II_b. The assertion made here is that this reflection band is the red-shifted III_b and that the weak II_b is completely obscured.

Turning again to the stretched film results for II summarized in Figure 6 and reinterpreting these data with a −30° orientation axis, then a consistent picture emerges for the three studies as shown at the bottom of Figure 6. Since the uncertainty range from the crystal spectra is excessive, we feel the best choice here is to use the value recalculated from the data of Matsuoka and Norden[17] on the basis of a −19° shift of their orientation axis. This value is $\theta_{II} = -46°$. The weak *b* axis component which is necessary for such an in-plane transition is that shown for II_b in

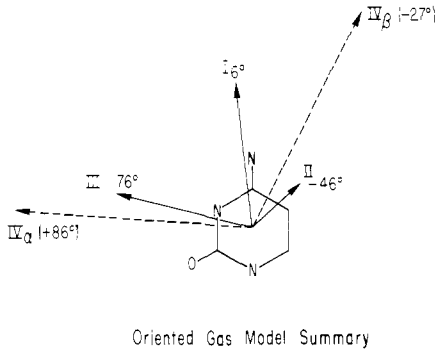

Figure 7. Final oriented gas transition moments for bands I to IV of cytosine. The two possible directions of IV are indicated as IV_α and IV_β.

Figure 2. This magnitude seems altogether reasonable.

Polarized fluorescence excitation can be used to estimate the angle between successive transition moments. Such measurements of 5-methylcytosine[9] give the angle between the moments of I and II as 40 ± 15°, and similar results have been given for cytidine monophosphate.[32] This value is (within the error) equivalent to the result of 52° for the angular difference in the assignments given here.

Transition III. The resolutions for III given in Figure 2 lead to two possible in-plane angles of +76° and −17°. The stretched film work[15-17] in this spectral region qualitatively indicates that the angle between I and III is larger than that between I and II, and on this basis we select the +76° direction for III. However, the LD results of Bott and Kurucsev[16] for cytosine, when modified as mentioned above, give a value for θ_{III} of 103° ± 4° and is 27° away from our selection.

Further reworking of Bott and Kurucsev's results for cytidine and cytidine monophosphate, where we make the assumption that I in both cases is close to the cytosine value of +6°, yields reasonable agreement in both systems for all bands. In the case of cytidine, the orientation axis must be at −9° rather than the reported −38°, and then we find $\theta_I = +6 \pm 27°$, $\theta_{II} = -44 \pm 5°$, and $\theta_{III} = +72 \pm 20°$. Agreement for CMP is obtained if the orientation axis is −7° instead of −38°, for then we find $\theta_I = +6 \pm 21°$, $\theta_{II} = -45 \pm 6°$, and $\theta_{III} = +64 \pm 28°$. The uncertainties are from the Bott and Kurucsev paper. It is noteworthy that these recalculated orientation axes are close to the axis between the amino and sugar (phosphate) groups. Such an orientation axis might be chosen on intuitive grounds based on molecular dimensions.

Transition IV. The strong band in the vicinity of 200 nm appears to have the directional choices of −27° or +86°. This ambiguity cannot be resolved for the transition is beyong the wavelength range of either fluorescence or linear dichroism studies. An investigation was made of the possibility of making a choice based on calculations of the strong energy shifts of the band components along the *a*, *b*, and *c* axes. Curiously, both choices gave equivalent results so that a distinction could not be made. The results for transitions I to IV are summarized in Figure 7.

Transition V and VI. In the region beyond 180 nm there are two features at 165 and 150 nm. Although this spectral region probably contains more than two transitions, the general intensity pattern resembles that for transition I. Plausible resolutions of this region into two in-plane polarized transitions can be made and are summarized in Table I along with the results for the other transitions.

Intermolecular Interactions

A description of the theory for treating intermolecular interactions in molecular crystals has been presented earlier.[10] The interactions cause crystal states of similar symmetry to mix. In addition to energy shifts, i.e., Davydov splittings, etc., what is observed is that the component intensities of each transition along the different axes change and that both the sign and magnitude of the change vary from axis to axis and face to face. The apparent transition moment vectors obtained directly from crystal dichroic ratios therefore can be very different from the true free molecule vectors.

A procedure for extracting free molecule parmeters from observed crystal spectra can be constructed by following an iterative procedure described in detail earlier.[10] In this procedure, the observed crystal components are used to identify the approximate orientation of the transition moment vectors for the several transitions. Dipole–dipole lattice sums are evaluated for these moments, and a full mixing calculation is carried through for each crystal axis separately. The calculated changes are applied in a reverse sense in order to obtain a first approximation to the oriented gas values. Another full exciton mixing calculation is carried through with the first approximate vector set, and the results are compared to the measured crystal spectra. The magnitudes of the components of the set of first approximate vectors are adjusted by subtracting the difference between the results of this mixing calculation and the experimental results. This corrected set constitutes the second approximate vector set. The process is reiterated until self consistency is attained, i.e., until a set of transition moment vectors is derived that yield the experimental band components in a full exciton mixing calculation. This derived set of vectors represents the free molecule transition moments. The original resolutions of the experimental spectra can be tailored within narrow limits, and the effects of choosing various alternate combinations of moment directions can be investigated.

In order to carry through the above procedure, dipole lattice sums for any two generally oriented transition dipoles situated at various combinations of unit cell sites must be evaluated many times. Since the interaction between any two arbitrarily directed dipoles can be simply expressed in terms of the interactions of their components along the various unit cell axes, we have for computational reasons chosen to use dipole sums of this nature. Table II gives the inner dipole sums evaluated with the Ewald procedure for unit dipoles (1 Å) directed along the unit cell axes of cytosine monohydrate.[33] Any particular dipole sum can be evaluated from the numbers listed; however, the appropriate

Table I. Crystal Data and Corresponding Oriented Gas Results[a,b]

	f_a	f_b	f_c	f^c	θ^d
I	0.06	0.35	0.02	0.14	+6 ± 2°
II	0.07	(0.02)	(0.02)	0.03	(−35) ± 30°
III	0.19	0.18	0.05	0.13	+76 ± 3°
IV	0.66	0.33	0.20	0.36	−26° or 86 ± 3°
V	0.10	0.35	(0.02)	0.15	~0° or ~60°
VI	0.12	0.45	(0.03)	0.20	~0° or ~60°

[a] All transition moments are directed within 0.5° of the molecular plane. [b] Values in parentheses are very uncertain. [c] Effective randomized value to be compared with the solution spectrum value. [d] Estimated uncertainties arise from the arbitrariness of the resolution of the spectra into band components.

Table II. Inner Dipolar Lattice Sums for Unit Vectors Directed Along the Various Unit Cell Axes[a-c]

	1,1	1,2	1,3	1,4
aa	−1127	−519	−453	1240
bb	−233	−585	−2455	−583
cc	−1190	−1078	327	−3293
ac	268	−871	178	497
ab	−0−	−989	−0−	−0−
bc	−0−	−1052	−0−	−0−

[a] Units are cm^{-1} $Å^{-2}$. [b] The dipole position is taken at the midpoint of the N_1–C_4 segment. The refined coordinates of ref 30 were used. [c] Equivalent site combinations are given as 3,4 = 1,2, 2,3 = 1,4, 2,4 = 1,3. Special cases are as follows: 3a,4b = −1a,2b; 3b,4c = −3b,4c. Also 1,1 = 2,2 = 3,3 = 4,4.

(32) Wilson, R. W.; Callis, P. R. *J. Phys. Chem.* **1976**, *80*, 2280.

(33) Born, M.; Huang, K. "Dynamical Theory of Crystal Lattices"; Clarendon: Oxford, England, 1954; p 248.

Table III. Typical Derived Free Molecule Transition Moment Parameters

	observed crystal[a]						derived free molecule[b]						free → crystal	
	f_a	f_b	f_c	f^c	θ, deg	ϕ, deg	f_a	f_b	f_c	f^c	θ, deg	ϕ, deg	$\Delta\theta$, deg	$\Delta\phi$, deg
I	0.06	0.35	0.01	0.14	+6	+2	0.07	0.24	0.02	0.11	+2	−2	−4	−4
II	0.07	0.02	0.01	0.03	−35	+6	0.06	0.01	0.02	0.03	−40	−5	−5	−11
III	0.19	0.18	0.03	0.13	+75	−4	0.17	0.15	0.05	0.11	+78	3	+3	+7
IV	0.66	0.33	0.26	0.38	−27	−4	0.66	0.37	0.22	0.38	−25	−2	+2	+2
V	0.10	0.35	0.02	0.15	+2	+3	0.06	0.21	0.00	0.10	+8	8	+6	+5
VI	0.12	0.45	0.03	0.20	+59	+2	0.19	0.80	0.02	0.33	55	14	−4	−6

[a] Values consistent with observed crystal spectra which lead to the derived results for the free molecule. [b] Depending on the various combinations of alternate choices of IV, V, and VI, the derived free molecule values of θ and ϕ for transitions I through IV vary over a range of 2° to 3° However, III is particularly sensitive to alternative choices of the nearby IV and can change by 8° in this regard. [c] Isotropic oscillator strength.

Table IV. Calculated and Observed Exciton Energies[a-c]

	E_a	E_b	E_c	E_{soln}[d]
I	37.9 (37.3)	36.5 (36.9)	38.1 (38.0)	37.5
II	43.0 (41.5)	42.9 (42.5)	43.2 (43.0)	43.0
III	45.4 (45.4)	44.7 (44.6)	46.0 (48.0)	45.2
IV	50.5 (51.2)	48.7 (48.9)	53.4 (55.0)	50.0
V	62.1	61.4	62.7	62.0
VI	65.9	63.7	66.8	65.0

[a] Units are 10^3 cm^{-1}. [b] Values in parentheses are observed crystal maxima. [c] No observed values for V and VI are given owing to the excessive arbitrariness of the resolution. [d] Aqueous solution spectrum values adjusted for the crystal shift. The values for V and VI are etimated from the thin film spectrum (see ref 31).

macroscopic term must be added for each case.

Convergence is rapid in the case of cytosine monohydrate, and self consistency is obtained in 10–12 iterations. No large changes are observed, and only minor tailoring of the experimental resolutions lead to derived transition moments that are reasonably close to being in-plane polarized. Since the various combinations of the vector choices for IV, V, and VI lead to slightly different results, we do not feel that further fine tuning of the calculation is in order. A typical result of an iterative calculation for a particular choice of the higher energy band polarizations is given in Table III. The calculations also yield the exciton energies of individual band components along the various axes. These energies are summarized in Table IV and for the most part agree nicely with the experimental values.

In spite of the fact that these calculations are approximate in that the number of transitions included is limited to six and terms other than transition dipole–transition dipole are excluded from consideration in the interaction, they were carried through with several goals: (1) to gauge the magnitudes of change in transition moment directions going from the free molecule to the crystal, (2) to obtain transition moment directions that are more nearly representative of the free molecule, and (3) to aid in the general spectral analysis by qualitative, if not quantitative, verification of energy shifts, etc.

The calculated angular changes $\Delta\theta$ and $\Delta\phi$ shown in Table III are of the order of 10° or less, while the derived free molecule transition moments are of the order of ±5° out-of-plane. Not surprisingly, the largest effects occur for the weakest transition II. Since a 5° out-of-plane cant produces a 1% intensity perpendicular to the molecular plane and at least a 1% intensity in orthogonal directions is expected to arise owing to vibronic mixing in the free molecule, we feel that further tailoring of the resolutions is not mandated under these circumstances.

The relatively small changes in θ between the derived free molecule transition moments and those derived by application of the oriented gas model directly to the crystal data indicate that crystal interaction effects are not large in these systems. The use of transition moments derived from crystal studies that have employed oriented gas model analyses is, therefore, not inappropriate in the calculation of the optical properties of other aggregates.

Discussion

A fairly complete assignment of the transitions of cytosine is now at hand, and it is useful to examine the theoretical calculations

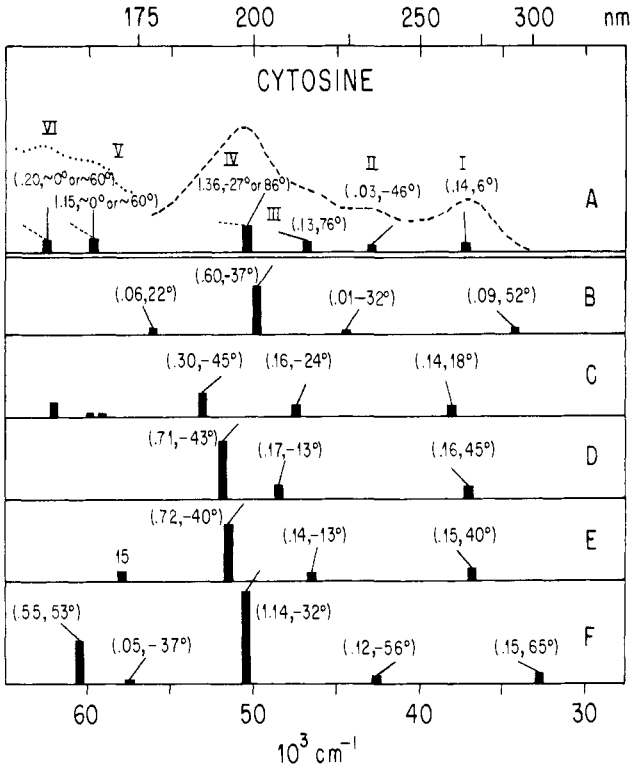

Figure 8. Comparison of experimental and theoretical results for the electronic spectrum of cytosine. [Top] Experimental results where the solid bars represent relative oscillator strengths and the lines atop the bars correspond to directions of θ (from the vertical). References for frames B through F are given as B (ref 35), C (ref 36), C (ref 37), E (ref 38), and F (ref 39). Redrawn from Callis, ref 14.

by comparing the experimental results with the various predictions of the spectrum.

Given the observed spectral features we can say there are no fewer than four transitions at wavelengths longer than 180 nm. The overall correlation of the crystal and solution spectra is good with the exception that the isotropic oscillator strength calculated from the crystal data of II is about 50% that estimated in solution. There appears to be but a single strong band in the 180–200 nm range, contrary to the results found earlier for a solution of cytosine in trimethylphosphate solvent.[34] We have retaken the spectrum using this solvent and find but one maximum in the higher energy region. No explanation is advanced for the disparity. The circular dichroism spectra of several cytidine derivatives given by Sprecher and Johnson[19] show features to be associated with bands I, II, and III. The CD curves in the 200-nm region show two peaks.

A comparison of several theoretical calculations with the present results is given in Figure 8.[35-39] All theoretical results yield two

(34) Clark, L. B.; Tinoco, I. *J. Am. Chem. Soc.* **1965**, *87*, 11.
(35) Srivastava, S. K.; Mishra, P. C. *Int. J. Quantum Chem.* **1979**, *16*, 1051.
(36) Hug, W.; Tinoco, I. *J. Am. Chem. Soc.* **1973**, *95*, 2803.
(37) Ito, H., l'Haya, Y. J. *Bull. Chem. Soc. Jpn.* **1976**, 3466.
(38) Danilov, V. I.; Pechenaya, V. I.; Zheltovsky, N. V. *Int. J. Quantum Chem.* **1980**, *17*, 307.

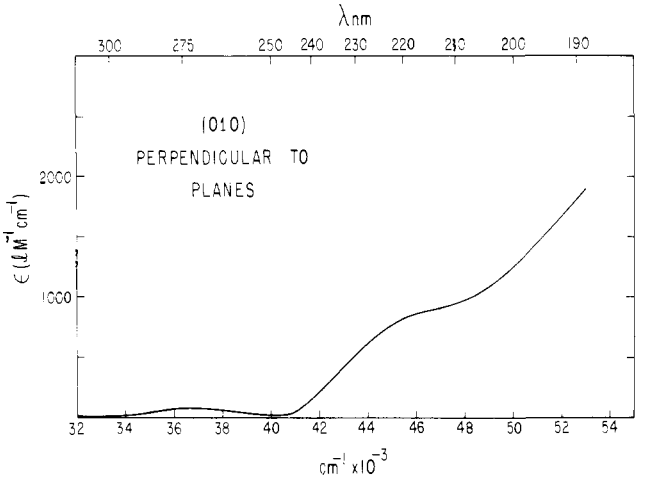

Figure 9. Absorption spectra polarized perpendicular to the molecular plane. The spectrum is derived from the reflection spectrum with light polarized perpendicular to the molecular plane on the (010) crystal face.

bands at wavelengths longer than 200 nm, and the calculated polarization directions of these transitions generally agree with the experimental results for I and II. The prediction of a single intense band in the vicinity of 200 nm with polarization θ in the range −30° to −40° is also unanimous. These results favor the experimental choice of −27° over the +86° as possibly the most likely. Where is band III in the theoretical calculations? The crystal spectra clearly show III to be a reasonably strong, in-plane polarized transition. The fact that it appears to be unaccounted for in all the theoretical calculations is itself difficult to account for.

Hug and Tinoco[40] predict a 256-nm position for the lowest perpendicularly polarized $n \rightarrow \pi^*$ band. $n \rightarrow \pi^*$ transitions are expected to be very weak with extinction coefficients not much larger than a few hundred at best. Such weak transitions are difficult to detect in the midst of strong in-plane bands even with the most favorable crystal symmetry as, for example, with light polarized exactly perpendicular to the molecular planes. The intensity of the formally in-plane, strong bands induced by either crystal imperfections or vibronic mixing is of the order of magnitude expected for $n \rightarrow \pi^*$ transitions. Nevertheless, in an attempt to locate any $n \rightarrow \pi^*$ bands, we have obtained a partial reflection spectrum (to 185 nm) from the *ac* face for light polarized perpendicularly to the molecular planes. The reflection is of the order of 3% between 330 and 185 nm. A very slight infection occurs in the vicinity of band I, while a slight maximum occurs at about 232 nm (43 000 cm^{-1}). The corresponding absorption spectrum is shown in Figure 9. The first feature transforms to a maximum crystal extinction coefficient of ~100 or less than about 1% than that observed along *b*, and no doubt corresponds to vibronically induced intensity of transition I. The second feature provides a band with peak height of the order of 800 at 220 nm (45 000 cm^{-1}). If this feature were derived from a perpendicularly polarized transition, then division by 3 gives the isotropic (solution) extinction coefficient. Although such a value is in the expected range for an $n \rightarrow \pi^*$ band, no definitive assignment can be made because, again, the intensity is about that to be expected of vibronically induced depolarization in the $\pi \rightarrow \pi^*$ transition III appearing at about the same energy.

Finally, we want to acknowledge the importance of the linear dichroism studies in resolving the ambiguities of the crystal spectra. The two methods are mutually supportive of each other. Both are necessary to resolve the ambiguities which arise in each. In addition, without some reduction in the possible choices for some of the transition moment directions, the treatment of crystal interactions would become unworkable.

Acknowledgment. L.B.C. thanks the participants of the First Mammoth Lakes Discussions on the Excited States of Nucleic Acid Constituents for their encouragement. This work was presented at the Euchem Conference on Molecular Orientation and Association held in Gothenburg, Sweden, June 1984. Prof. Bengt Norden, Prof. Tom Kurucsev, and Dr. Yukio Matsuoka are thanked for helpful discussions. Large teaching loads at UCSD substantially delayed publication of this research.

Registry No. Cytosine, 71-30-7.

(39) Srivastava, S. K.; Mishra, P. C. *Int. J. Quantum Chem.* **1980**, *18*, 827.
(40) Hug, W.; Tinoco, I. *J. Am. Chem. Soc.* **1974**, *96*, 665.